Supporting Information

In situ generated Fe_3C embedded Fe-N-doped carbon nanozymes with enhanced oxidase mimic activity for total antioxidant capacity assessment

Rui Li[+], Xiaohong Qiao[+], Huijun Ma, Hanmei Li, Cong Li and Lihua Jin[*]

Key Laboratory of Synthetic and Natural Functional Molecule Chemistry of the Ministry of Education, College of Chemistry & Materials Science, Northwest University, Xi'an 710069, People's Republic of China

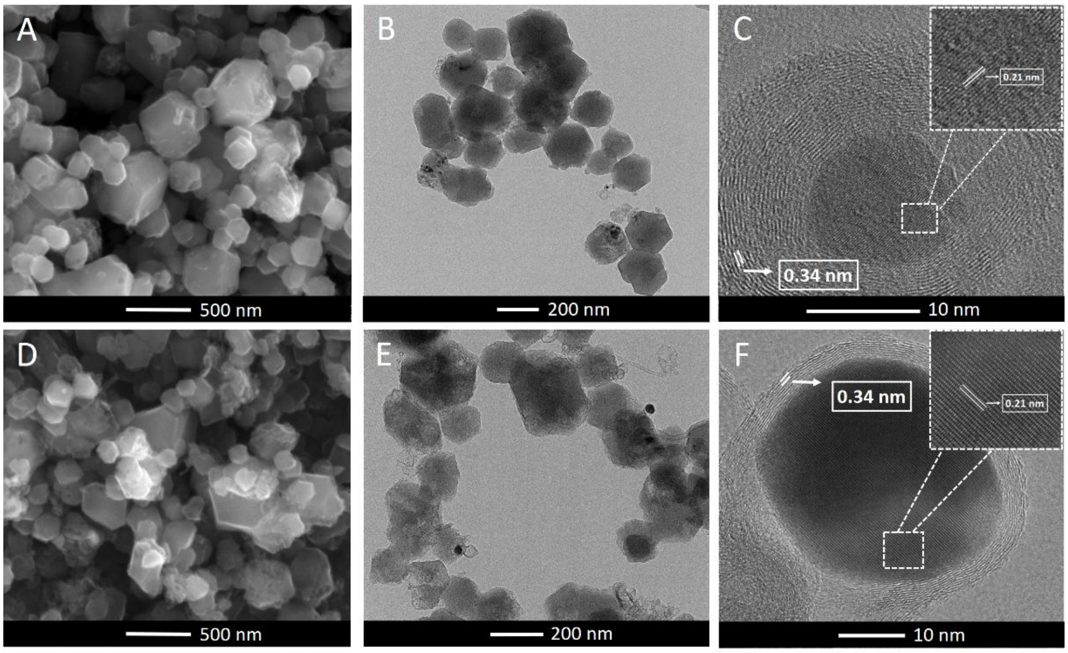

Fig. S1 SEM image, TEM image and HRTEM image of CMs-700 (A-C) and CMs-900(D-E).

[*] To whom correspondence should be addressed. Fax: +86-029-88302635. E-mail: jinlihua@nwu.edu.cn.

[+] These authors contributed equally.

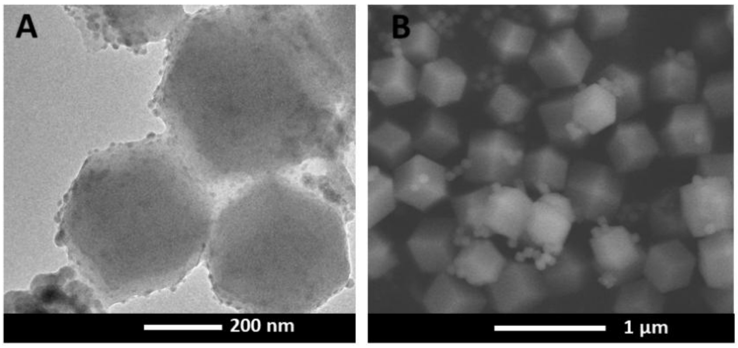

Fig. S2 SEM image (A) and TEM image (B) of ZIF framework

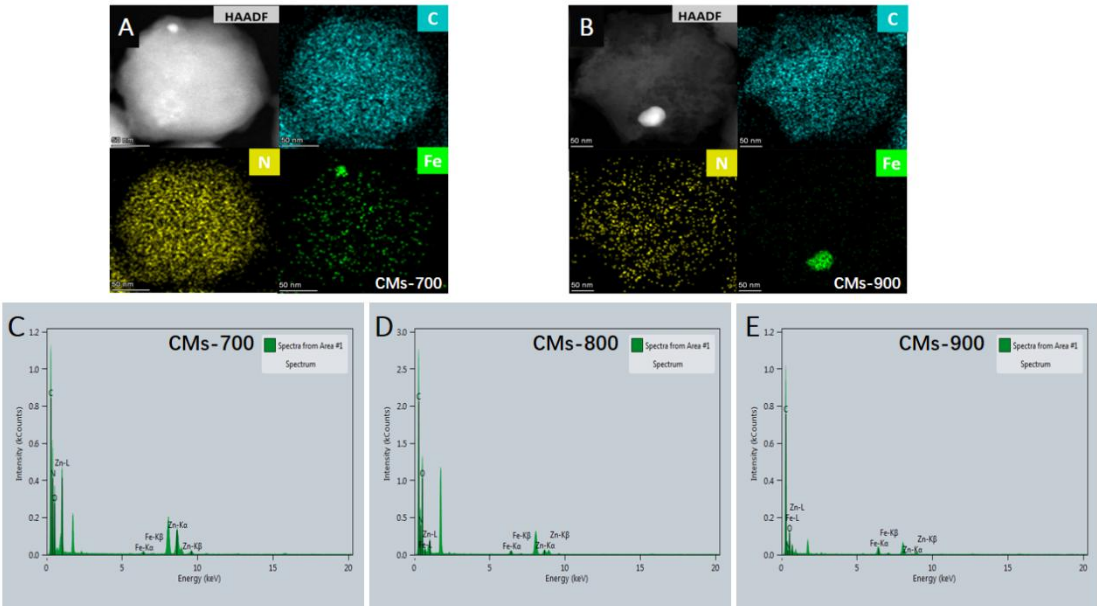

Fig. S3 Element mappings of CMs-700 **(A)** and CMs-800 **(B)**; EDS images of CMs-700 **(C)**, CMs-800 **(D)** and CMs-900**(E)**.

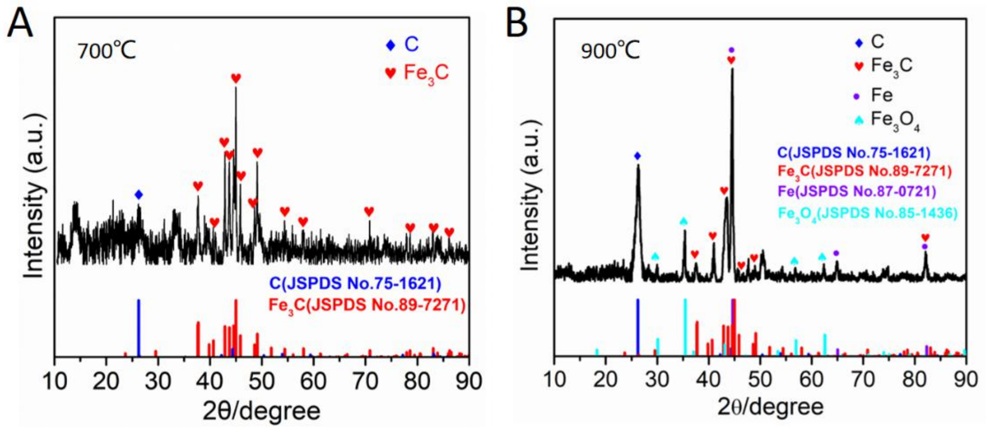

Fig. S4 XRD patterns of CMs-700 **(A)** and CMs-900 **(B)**.

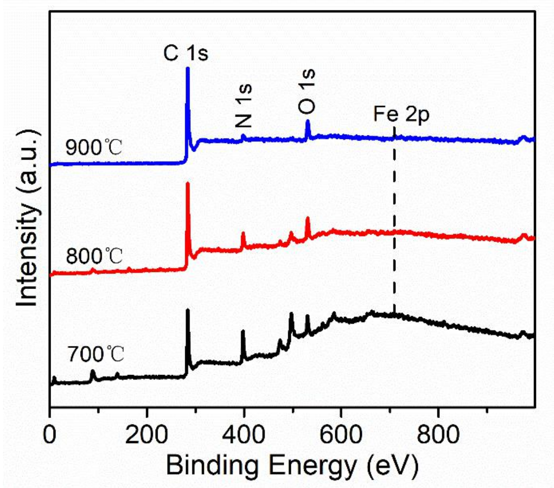

Fig. S5 The overview XPS spectra of the CMs-700, CMs-800 and CMs-900.

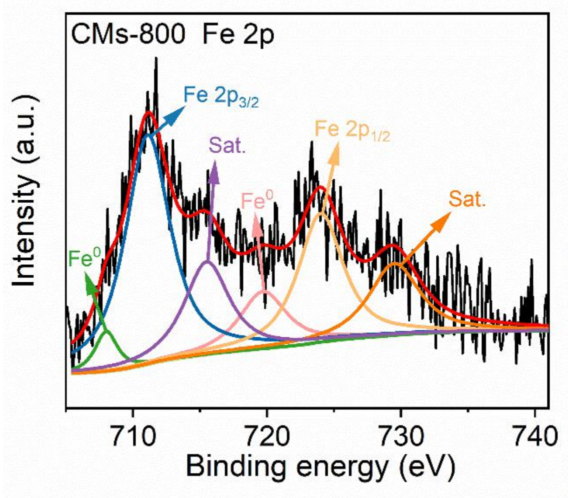

Fig. S6 High-resolution XPS Fe 2p spectra of CMs-800

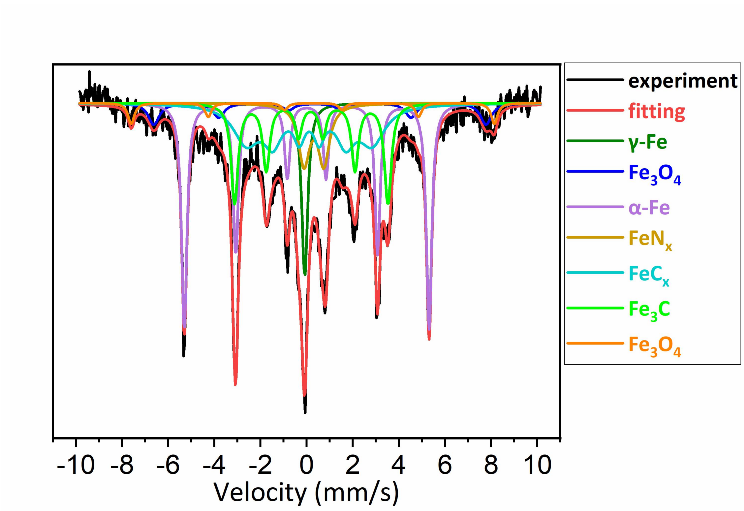

Fig. S7 ^{57}Fe Mössbauer fitted parameters of CMs-800

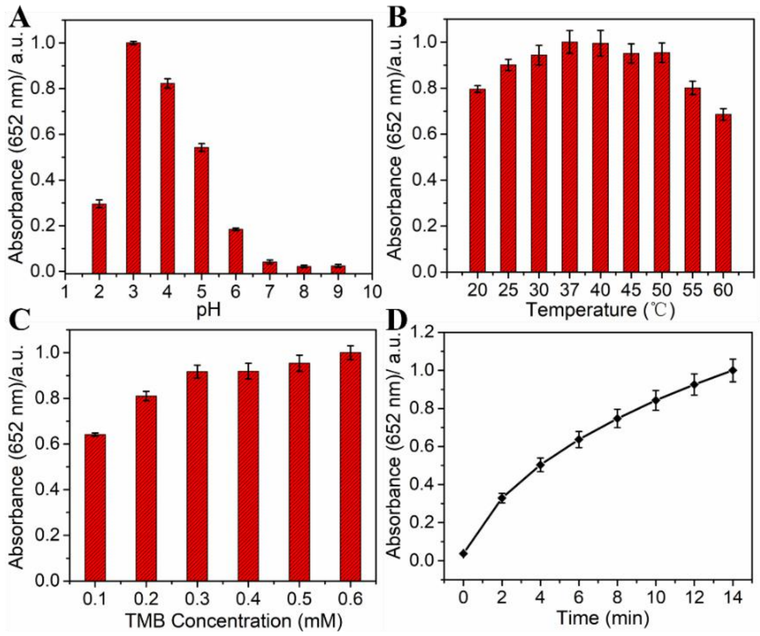

Fig. S8 The effects of reaction condition on the oxidase mimic activity of CMs-800 **(A)** pH; **(B)** temperature; **(C)** TMB concentration; **(D)** reaction time.

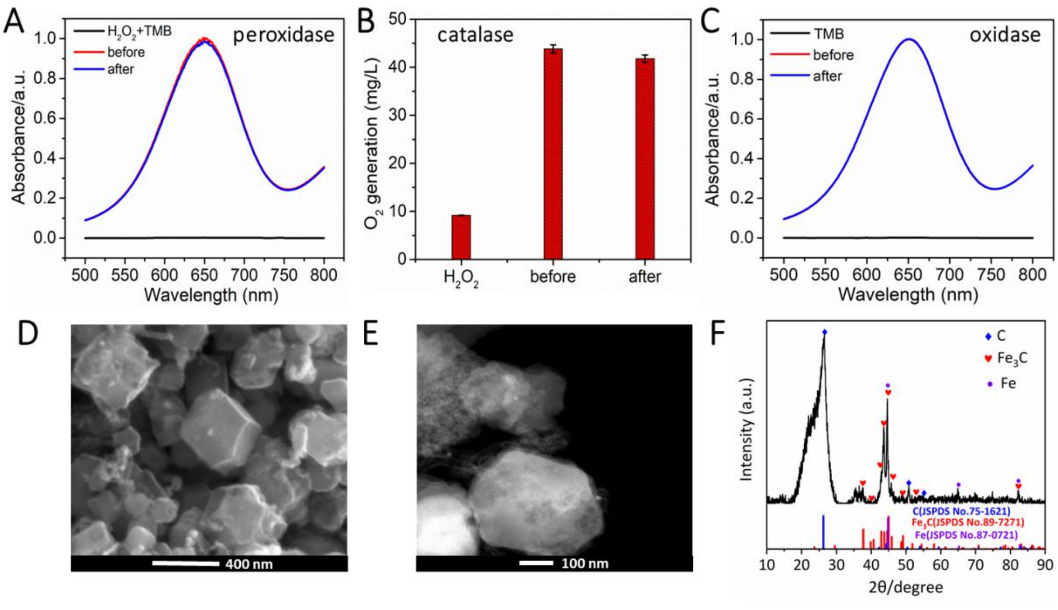

Fig. S9 (A-C) The comparison of peroxidase-like, catalase-like and oxidase-like activities of CMs-800 before and after acid leaching experiment; **(D-F)** the SEM image, TEM image and XRD data of CMs-800 after acid leaching experiment.

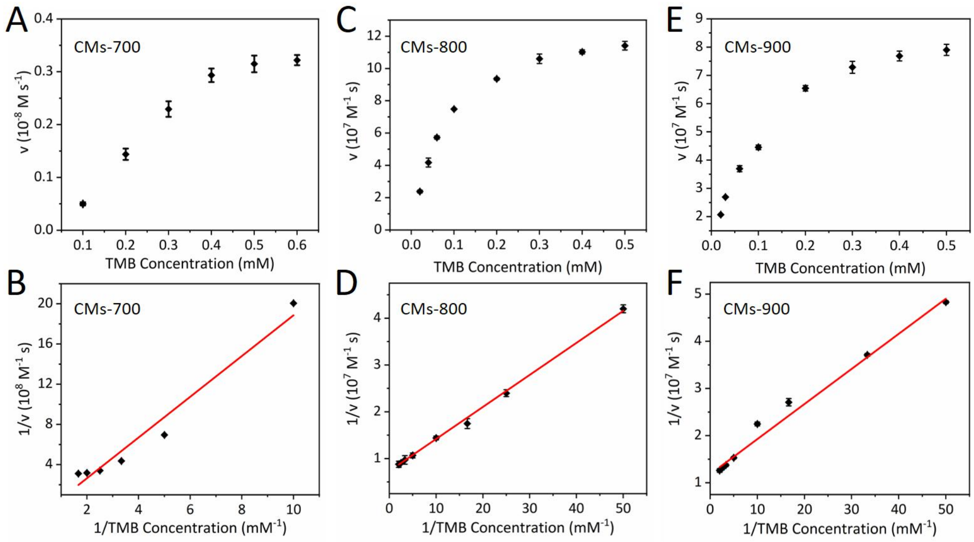

Fig. S10 Oxidase mimic steady-state kinetic assay of the CMs-700**(A)**, CMs-800**(C)** and CMs-900**(E)** for TMB. Line weaver-Burk plot of CMs-700**(B)**, CMs-800**(D)** and CMs-900**(F)** for the variation of TMB.

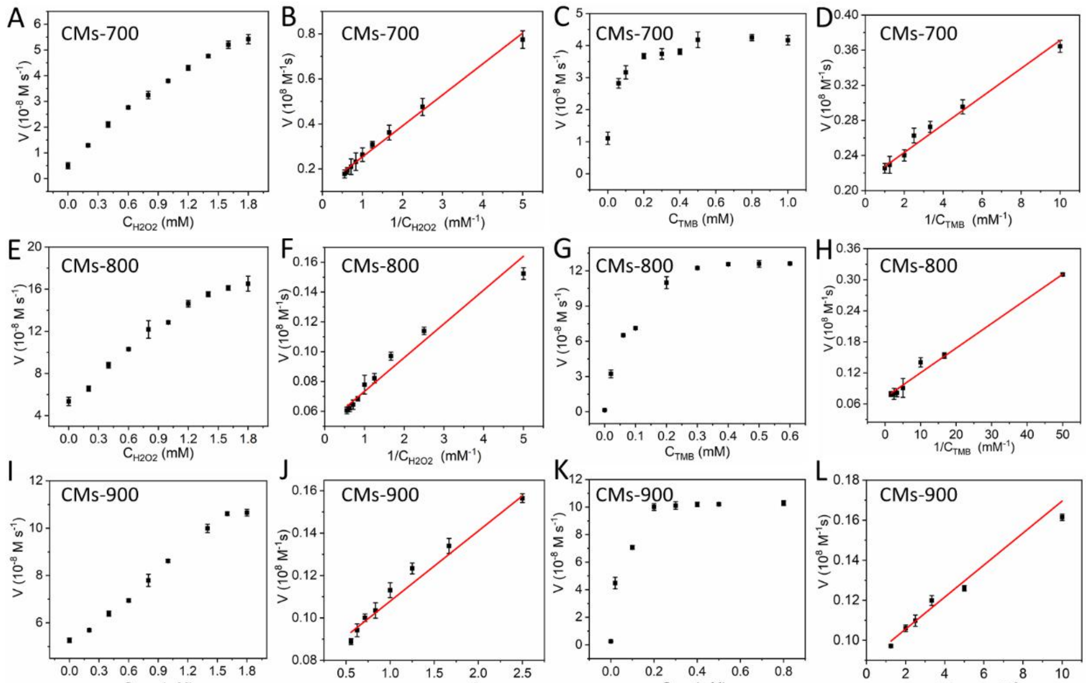

Fig. S11 Peroxidase mimic steady-state kinetic assay of the CMs-700**(A)**, CMs-800**(E)** and CMs-900**(I)** for H_2O_2; Line weaver-Burk plot of CMs-700**(B)**, CMs-800**(F)** and CMs-900**(J)** for the variation of H_2O_2; peroxidase mimic steady-state kinetic assay of the CMs-700**(C)**, CMs-800**(G)** and CMs-900**(K)** for TMB; Line weaver-Burk plot of CMs-700**(D)**, CMs-800**(H)** and CMs-900**(L)** for the variation of TMB.

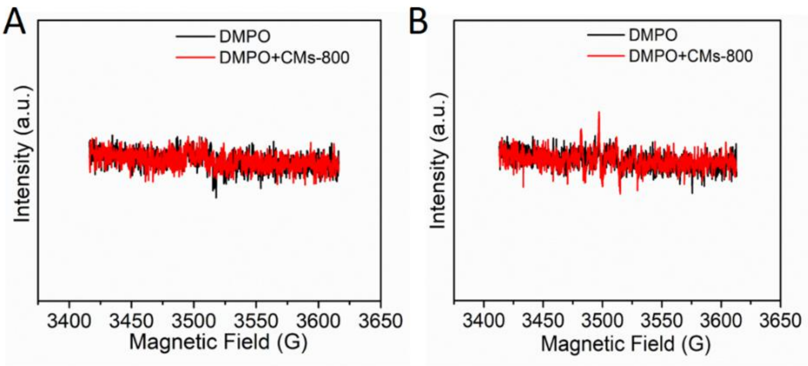

Fig. S12 The EPR spectra of the **(A)** DMPO+CMs-800 aqueous solution, and **(B)** DMPO+CMs-800 methanol solution.

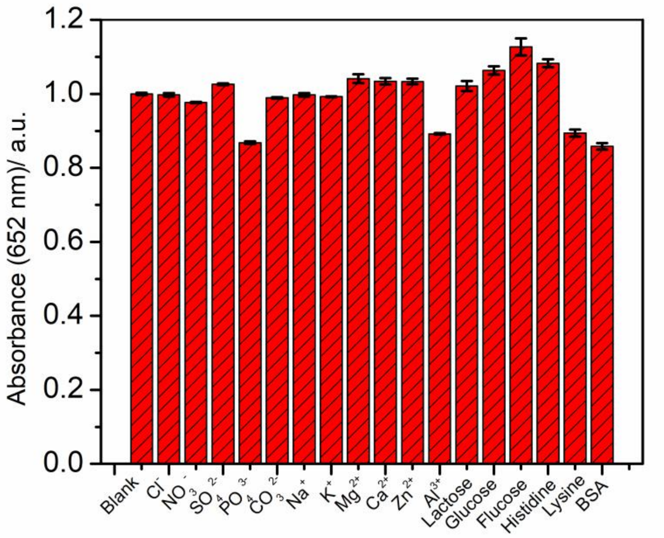

Fig. S13 Selectivity of AA sensing system for common anions, cations and small molecules. All common anions, cations and small molecules were 1mM except BSA was 0.1 mg/mL.

Table S1. ^{57}Fe Mössbauer fitted parameters of CMs-800.

Catalyst	IS($mm\cdot s^{-1}$)	QS($mm\cdot s^{-1}$)	H(T)	Phase
CMs-800	0.18785	0.02730	20.66	Fe_3C
	0.1114	~	16.96	FeC_x
	0.31537	0.864	~	FeN_x
	0.00099	~	33.00	α-Fe
	0.46536	0.22015	44.78	tetahed B-site of Fe_3O_4
	0.27929	-0.02579	48.94	tetahed A-site of Fe_3O_4

Table S2 Comparison of oxidase-like steady-state kinetic parameter for Fe_3C@Fe-N-CMs and other oxidase mimics.

Nanozyme	Substrate	K_m(mM)	v_{max}(10^{-8} M s^{-1})	[E](μg/mL)	Reference
N-PCNSs-3	TMB	0.084	0.42	25	[1]
Fe SAEs		0.13	2.25	20	[2]
CeO_2NRs-MOF/Cr(VI)		0.108	0.977	1000	[3]
Iron alkoxide		0.12	2.11	—	[4]
Fe-Co-LDH		0.34	5.4	33	[5]
MOF(Co/2Fe)		0.199	0.39	20	[6]
Pt NCs		0.63	2.7	—	[7]
AWNRs-9		0.109	2.17	50	[8]
Nanoceria		0.42	10.04	5×10^{-5}	[9]
Fe/NC-800		0.170	8.9	5.0	[10]
Commercial Pt/C		0.129	5.2	—	[11]
FeN_5 SA/CNF		0.148	75.8	5.0	
CMs-700		1.4	0.7	2.0	This work
CMs-800		0.095	14.1	2.0	This work
CMs-900		0.063	8.5	2.0	This work

K_m is the Michaelis constant, v_{max} is the maximal reaction velocity and k_{cat} is the catalytic constant, where $k_{cat} = v_{max}/[E]$, [E] is the molar concentration of metal in nanozymes.

Table S3. The peroxidase-like enzyme kinetic parameters of Fe_3C@Fe-N-CMs

Catalyst	K_m (mM)		v_{max} (10^{-8}M s^{-1})		[E](μg/mL)
	TMB	H_2O_2	TMB	H_2O_2	
CMs-700	1.183	1.183	4.73	8.66	2.0
CMs-800	0.0651	0.447	18.70	19.73	2.0
CMs-900	0.0893	0.442	11.13	13.37	2.0

K_m is the Michaelis constant, v_{max} is the maximal reaction velocity and k_{cat} is the catalytic constant, where $k_{cat} = v_{max}/[E]$, [E] is the molar concentration of metal in nanozymes.

Table S4. Recovery experiment of AA in diluted commercial vitamin drink

Sample	**Original (μM)**	**Added (μM)**	**Found (U/L)**	**Recovery (%)**	**RSD(%, n=3)**
1	67.92	10.00	10.16	101.6	3.5
2	67.92	20.00	20.54	102.7	2.8
3	67.92	30.00	30.38	101.3	4.3

Reference

[1] K. Fan, J. Xi, L. Fan, P. Wang, C. Zhu, Y. Tang, X. Xu, M. Liang, B. Jiang, X. Yan and L. Gao,In vivo guiding nitrogen-doped carbon nanozymefor tumor catalytic therapy. *Nat.Commun.*, **2018**, 9,1440.

[2] Wang, M. K.;Zhou, X. B.; Wang, S.; Xie, X. L.; Wang, Y. F.; Su, X. G., Fabrication of bioresource-derived porous carbon-supported iron as an efficient oxidase mimic for dual-channel biosensing. *Anal. Chem.*, **2021**, 93, 3130-3137.

[3] Wan, G.Y.; Liang, R. P.; Qiu, J. D., Nanoceria-templated metal organic frameworks with oxidase-mimicking activity boosted by hexavalent chromium. *Anal. Chem.*, **2020**, 92, 2339-2346.

[4] Xu, X. C.; Luo, J. L.; Wei, S. T.; Zou, X. B.; Niu, X. H.; Pan, J. M., Three-dimensional flower-like multifunctional adsorbents with excellent sorptive removal and colorimetric detection of arsenate. *Chem. Eng. J.*, **2020**, 398, 125649.

[5] Xu, X. C.; Zou, X. B.; Wu, S. W.; Wang, L. J.; Pan, J. M.; Xu, M. J.; Shan, W.; Li, X.; Niu, X. H., Colorimetric determination of As(III) based on 3-mercaptopropionic acid assisted active site and interlayer channel dual-masking of Fe-Co-layered double hydroxides with oxidase-like activity. *Microchim. Acta*, **2019**, 186,815.

[6] Yang, H. G.; Yang, R. T.; Zhang, P.; Qin, Y. M.; Chen, T.; Ye, F. G., A bimetallic (Co/2Fe) metal-organic framework with oxidase and peroxidase mimicking activity for colorimetric detection of hydrogen peroxide. *Microchim. Acta*, **2017**, 184, 4629-4635.

[7] Yu, C. J.; Chen, T. H.; Jiang, J. Y.; Tseng, W. L., Lysozyme-directed synthesis of platinum nanoclusters as a mimic oxidase. *Nanoscale*, **2014**, 6, 9618-9624.

[8] Ju, P.; Wang, Z.; Zhang, Y.; Zhai, X. F.; Jiang, F. H.; Sun, C. J.; Han, X. X., Enhanced oxidase-like activity of $Ag@Ag_2WO_4$ nanorods for colorimetric detection of Hg^{2+}. *Colloids Surfaces A*, **2020**, 603, 125203.

[9] Cheng, H. J.; Lin, S. C.; Muhammad F.; Lin, Y. W.; Wei, H., Rationally modulate the oxidase-like activity of nanoceria for self-regulated bioassays. *ACS Sensors*, **2016**, 1, 1336-1343.

[10] Chen, Q.M.; Liang, C.H.; Zhang, X.D.; Huang, Y.M.; High oxidase-mimic activity of Fe nanoparticles embedded in an N-rich porous carbon and their application for sensing of dopamine, *Talanta*, **2018**, 182, 476-483.

[11] Huang, L.; Chen, J.X.; Gan, L.F; Wang, J.; Dong, S.J.; Single-atom nanozymes, *Sci. Adv.***2019**, 5 , eaav5490.